ERDC/CHL MP-21-4

US Army Corps
of Engineers®
Engineer Research and
Development Center

The Response of Vegetated Dunes to Wave Attack

Duncan B. Bryant, Mary Anderson Bryant, Jeremy A. Sharp,
Gary L. Bell, and Christine Moore

August 2021

Coastal and Hydraulics Laboratory

The U.S. Army Engineer Research and Development Center (ERDC) solves the nation's toughest engineering and environmental challenges. ERDC develops innovative solutions in civil and military engineering, geospatial sciences, water resources, and environmental sciences for the Army, the Department of Defense, civilian agencies, and our nation's public good. Find out more at www.erdc.usace.army.mil.

To search for other technical reports published by ERDC, visit the ERDC online library at https://erdclibrary.on.worldcat.org/discovery.

ERDC/CHL MP-21-4
August 2021

The Response of Vegetated Dunes to Wave Attack

Duncan B. Bryant, Mary Anderson Bryant, Jeremy A. Sharp, Gary L. Bell, and Christine Moore

Coastal and Hydraulics Laboratory
U.S. Army Engineer Research and Development Center
Field Research Facility
3909 Halls Ferry Road
Vicksburg, MS 39180

Final report

Prepared for U.S. Army Corps of Engineers
Washington, DC 20134

Under USACE Flood and Coastal Systems Program, Coastal Inlets Program, DOER (EWN) Program

Preface

This study was conducted for the U.S. Army Corps of Engineers (USACE) under the USACE Flood and Coastal Systems Program led by Dr. Julie Rosati and Ms. Mary Cialone, the Coastal Inlets Research Program led by Ms. Tanya Beck, and the Engineering with Nature Initiative within the Dredging Operations and Environment Research Program led by Dr. Todd Bridges.

The work was performed by the U.S. Army Engineer Research and Development Center, Coastal and Hydraulics Laboratory (ERDC-CHL). At the time of publication of this paper, the Deputy Director of ERDC-CHL was Mr. Keith Flowers, and the Director was Dr. Ty V. Wamsley.

This article was originally published online in *Coastal Engineering* on 13 May 2019.

Mr. Marshall Thomas and Mr. William Henderson provided laboratory support. The authors would also like to thank the reviewers for their time and input.

The Commander of ERDC was COL Teresa A. Schlosser and the Director was Dr. David W. Pittman.

The response of vegetated dunes to wave attack

A B S T R A C T

For many coastal communities, dunes serve as the primary defense against tropical and extratropical events. Vegetation is believed to increase the stability of dunes during wave attack, but limited data is available. A physical model study was performed to evaluate changes in the dune stability with and without biomass, both above and belowground. The above and belowground biomass was modeled using wooden dowels and coir fibers, respectively. For both the collision and overwash storm impact regimes, the results of this study clearly demonstrate that the inclusion of biomass in the model dune reduces the erosion and overwash. The combination of both above and belowground biomass was the most effective at reducing erosion followed by belowground biomass, with aboveground biomass providing the smallest benefit regardless of the wave condition and water level. Additionally, the overwash of sediment and water was decreased with the inclusion of biomass, following the same trends as the erosion. As the dune eroded, the storm impact regime transitioned from collision to overwash. The inclusion of biomass delays this transition in storm impact regime, providing greater protection to coastal communities. This study highlights the need to consider dune vegetation for dune construction and coastal planning.

1. Introduction

Out of the 7.8 million km^2 of land in the United States, less than 10% is classified as coastal shoreline counties, which are counties adjacent to open ocean, major estuaries, and the Great Lakes. In 2010, 39% of the nation's population lived in these counties, a population density over six times greater than inland counties. The population in these areas is projected to increase by 10 million residents, an 8% increase, by 2020 (NOAA, 2013). These highly populated counties are most vulnerable to the full range of effects from coastal hazards, particularly those associated with tropical and extratropical cyclones. Furthermore, these communities may experience greater pressures due to inflating population, sea level rise, and a possible change in projected storm frequency and/or intensity.

One platform to foster sustainable coastal communities is the adoption of adaptable, nature-based defenses into the planning process. One example of a natural feature known to provide some level of protection is coastal foredunes (Hesp, 2002; Davidson-Arnott 2005, 2010; Borsje et al., 2011; Van Slobbe et al., 2013). Damage assessments following Hurricane Sandy in 2012 showed communities fronted by dune systems (e.g., Sea Girt, NJ; Rockaway Peninsula, NY) sustained fewer damages as a direct result of reduced overland surge propagation, wave battering, and/or severe scour (Walling et al., 2014; City of New York, 2013; USACE, 2013). Yet, many foredune systems are in advanced stages of degradation or may have been actively removed to create aesthetic views and allow beachfront property development (Hanley et al., 2014; Sigren et al., 2014). Now recognizing the dynamic infrastructure offered by foredune systems, many shore communities are engaging in efforts to construct and rehabilitate dunes to enhance coastal protection.

An important step in the dune restoration and preservation process is planting vegetation. Guidelines for constructing and restoring dunes tout vegetation as critical for slowing wind speeds to encourage deposition and prevent aeolian remobilization of the sediment (Knutson, 1977; Texas General Land Office, 2005; Williams, 2007). While the role of vegetation in dune evolution is well studied (Arens, 1996; Arens et al., 2001, Keijsers et al., 2015, Keijsers et al., 2016), the value of this same vegetation in supporting dune survivability during episodic erosional hydrodynamic events is undetermined. Empirical data to gain a mechanistic understanding of how, and to what degree, vegetation may impact dune erosion due to waves is lacking, with hypothesized understanding relying largely on anecdotal evidence, post-hoc observational studies, and findings extrapolated from other environments (City of New York, 2013; Donnelly et al., 2006; Feagin et al., 2015). In

particular, aquatic and riparian vegetation is known to attenuate flow energy aboveground (Bonham, 1983; Anderson and Smith, 2014; Gedan et al., 2011) and reinforce sediment belowground (Miller and Jastrow, 1990; Pollen, 2007; Veylon et al., 2015). These functions are thought to extend to dune vegetation exposed to wave attack.

Originally developed for categorizing storm impacts to dunes, the regimes defined by Sallenger (2000) may be extrapolated to determine the plant structures reached by waves. The possible regimes that directly impact dune vegetation include wave collision, wave overwash, and wave inundation. Focus herein will be on the collision and overwash regimes. While the collision and overwash regimes proposed by Sallenger (2000) have been studied extensively in large-scale experiments (Kraus and Smith, 1994; Van Thiel de Vries, 2008; Van Rijn, 2009; Tomasicchio et al., 2011; Figlus et al., 2011), laboratory studies of these same regimes that also account for vegetation are extremely limited. To the authors' knowledge, only three laboratory studies exploring the protective role of coastal dune vegetation are published.

Kobayashi et al. (2013) conducted a small-scale flume experiment to examine the effects of woody plants, represented by a highly simplified model of buried wooden dowels, on dune erosion and overwash. Two dune profiles were modeled, a high dune to examine wave overtopping, overwash, and scarping and a low dune to examine only wave overtopping and overwash. For the high dune, the dowels reduced scarping, delayed initiation of wave overtopping, and reduced overtopping and overwash rates compared to the bare dune when the cross-shore distance of the vegetation zone was expanded seaward from the lee slope to the stoss slope. A decrease in wave overtopping and overwash was also observed for the low dune with seaward vegetation. The dune profiles, wave overtopping, and sand overwash rates were used by Ayat and Kobayashi (2015) to expand the one-dimensional cross-shore model CSHORE to wooded dunes. Dune evolution with and without dowels were predicted within a factor of about 2. CSHORE predicted the measured trends in wave overtopping and overwash but showed difficulty in predicting rate magnitudes. Additional experiments, supported by model results, showed that the effectiveness of the dowels in reducing dune erosion and overwash diminished when the ratio of cylinder spacing to diameter exceeded 7 or after toppling of the dowels on the stoss slope.

Figlus et al. (2014) and Silva et al. (2016) conducted small-scale flume experiments using live vegetation. Figlus et al. (2014) modeled only the collision regime while Silva et al. (2016) explored the swash, collision, and overwash regimes. The vegetation, *S. virginicus* in Figlus et al. (2014) and *I. pes-caprae* in Silva et al. (2016), were grown in greenhouses and transplanted into model dunes for testing. Immature *S. virginicus* (2 weeks old) had a relatively small effect in reducing the eroded dune volume, whereas the most mature (5 weeks old) and densely planted *S. virginicus* reduced the total eroded dune volume by 8% for irregular waves and 30% for regular waves. Testing of substrate samples with no roots, 6-week-old, and 9-week-old plant roots showed an increase in the ultimate shear strength of the substrate with more mature root systems (Figlus et al., 2014). Silva et al. (2016) observed a reduction in dune erosion for vegetated dunes compared to dunes without vegetation regardless of the wave condition, morphology of the beach-dune profile, and mode of erosion, although results were qualitative to some extent. Accounting for belowground biomass in future research was stressed by both Figlus et al. (2014) and Silva et al. (2016).

This paper presents a laboratory study to further quantify the engineering services dune vegetation, both above and belowground biomass, provides in reducing the erosion of dunes due to wave attack. Section 2 introduces the physical model, including the hydrodynamic conditions and vegetation biomass covers. The results in Section 3 detail changes in the erosion and overwash due to the inclusion of biomass. Finally, the presented results are framed in the context of natural and constructed dunes, with future consideration and research needs highlighted in Section 4.

2. Experiment description

2.1. Laboratory setup

The experiment was performed at the U.S. Army Engineer Research and Development Center in Vicksburg, Mississippi in a 63.4-m long, 1.5-m wide, and 1.5 m-deep concrete wave flume equipped with an electro-hydraulic piston wave generator. The wavemaker does not have the capability to absorb reflected waves. The deep section housing the wave paddle is 5.4-m long, followed by a 1:44 slope for 19.5 m that leads to 26.8 m long flat testing area with the far 12.2 m section having viewing glass. A 1:15 beach-dune model was constructed in this testing area, beginning approximately 43.9 m from the wave board at rest. The sand comprising the beach-dune model was well-sorted with a median diameter D_{50} of 0.15 mm. In order to reduce the amount of cross-shore transport and minimize rebuilding during testing, the beach was designed to an equilibrium profile with a profile scale factor, A, of 0.084 $m^{1/3}$(Dean and Dalrymple, 2004). The equilibrium beach measured 6.6 m long and no offshore bar was formed during testing. The dune, measuring 1.13 m long and 49.8 cm high relative to the flume floor, was constructed landward of the beach and is similar in profile to Kobayashi et al. (2013). The foreslope and backslope of the dune are 25° and 20°, respectively. The dune terminated at an impermeable, sloping wall located 51.7 m from the wave board. The sloping wall, measuring 37.1 cm above the flume floor, was constructed below the elevation of the dune crest to allow for the collection of both sediment and water overwash. The entire length of the beach-dune model was approximately 7.8 m. Water surface elevations were measured with 10 Akamina AWP-24 capacitance wave staffs (WS) sampling at 25 Hz. The locations of the wave staffs from the wavemaker at rest were the following: 6.8, 7.1, 7.7, 29.7, 43.8, 46.8, 48.8, 49.8, 50.3, and 50.7 m along the centerline of the flume. The three offshore wave staffs (those closest to the wave paddle; WS 8–10) were 100 cm long and served as a Goda array to measure wave reflection. The nearshore staffs (WS 1–7) were 60 cm long. Fig. 1 diagrams the beach-dune model and wave staff locations.

2.2. Hydrodynamic conditions

Two water levels were modeled, a still water level (SWL) of 30.0 cm and a deeper SWL of 35.0 cm, denoted by letters S and D in the testing

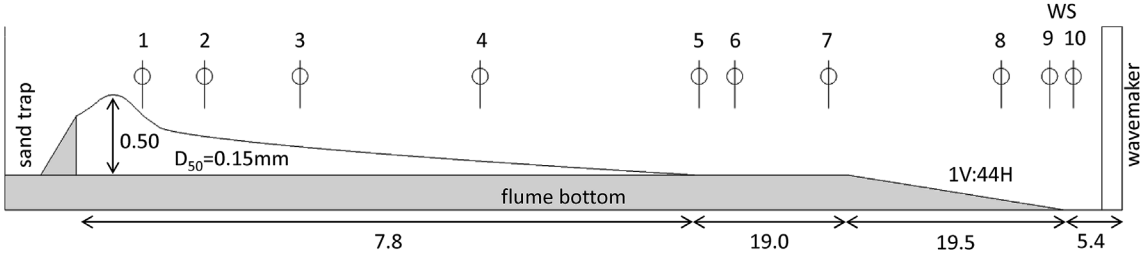

Fig. 1. Setup of beach-dune model (not drawn to scale). The white numbered circles denote the location of the wave staffs.

matrix, respectively. These water levels were measured relative to the toe of the beach, such that the maximum dune elevation over the SWL was 19.8 cm for the S condition and 14.8 cm for the D condition. Irregular wave spectra were generated using a TMA shallow-water spectrum with a gamma value of 3.3. Guided by the storm impact scale proposed by Sallenger (2000), the two regimes targeted were the collision and overwash regimes. The collision regime occurs when the 2% exceedance runup elevation is greater than the elevation of the dune base but not the dune crest whereas the overwash regime is characterized by a 2% exceedance elevation greater than the dune crest but not continuously inundated. The durations of the wave bursts for the collision and overwash conditions, denoted C and O henceforth, were 1200 s and 400 s, respectively. The wave spectral density *S(f)* at each wave staff was computed from the demeaned water surface elevation timeseries using a fast Fourier transformation. The local zero-moment wave height H_{m0} was estimated from the wave spectra using the following relationship:

$$H_{m0} = 4\sqrt{\sum_{n=1}^{N} S(f_n)\Delta f} \tag{1}$$

The local peak wave period T_p was extracted directly from the spectra. Except for the DO wave condition, each hydrodynamic condition consisted of three identical wave bursts impinging on the dune.

A total of five hydrodynamic conditions were modeled, three at the S SWL and two at the D SWL. The integral wave parameters given in Table 1 are those at WS 10, the gauge closest to the wavemaker. Incident and reflected waves were separated by applying a three gauge separation technique based on the method of Goda and Suzuki (1976) to the timeseries of WS 8–10. The reflection coefficient *Kr* ranged from a minimum of 0.18 for the SC2 condition to a maximum of 0.57 for the DC condition. Because each condition consisted of multiple wave bursts, the average incident H_{mo} and its standard deviation σ are provided. Incident wave heights range from 4.3 cm to 13.2 cm and were selected to ensure the target storm impact scale was modeled. The standard deviation of H_{mo} was very small, about 1 mm, indicating high repeatability of the wave bursts. The target peak period T_p was informed by measurements taken with a Nortek AWAC set in a water depth of 6 m at the US Army Field Research Facility in Duck, North Carolina. During the time period of 05:00 GMT 28 October 2012 to 13:00 GMT 29 October 2012 as Hurricane Sandy passed to the East, hourly measured peak periods ranged between 12.7 and 16.06 s. Corresponding to the average peak period of these field measurements T_p = 14.3 s, a peak period of 3.69 s was chosen for all hydrodynamic conditions, except SC2. A model peak period of 2.0 s (7.7 s in the prototype) was chosen for SC2 to provide a contrasting condition. The hydrodynamic conditions given in Table 1 were repeated for a dune without vegetation (control), with isolated aboveground biomass (A), with isolated belowground biomass (B) and, lastly, with a combination of above and belowground biomass (AB). Data was collected for a total of 76 wave bursts, including repeats of the non-vegetated, control dune.

Table 1
Modeled hydrodynamic conditions. The still water level (SWL) is relative to the toe of the beach whereas H_{mo} and T_p are the incident wave conditions measured at WS 10.

	SWL (cm)	H_{m0} (cm)	σ (cm)	T_p (s)	K_r	Number of Wave Burst	Duration of Wave Burst (s)
SC1	30	7.4	0.10	3.69	0.38	3	1200
SC2	30	8.4	0.06	2.0	0.18	3	1200
SO	30	12.8	0.11	3.69	0.28	3	400
DC	35	4.3	0.10	3.69	0.57	3	1200
DO	35	13.2	0.12	3.69	0.34	1*	400

*Note: The DO-AB number of runs was later expanded to 3.

2.3. Plant characteristics

To build a representative physical model of a natural dune system that also addressed the inherent complexities associated with scale (e.g., Silva et al., 2016), the beach-dune model employed artificial vegetation founded on measured plant characteristics. The scaled model considered both above and belowground biomass of dune vegetation, both in isolation and in combination (Fig. 2) in order to investigate the interaction between the vegetation structure and erosion.

In the beach-dune model, aboveground biomass (A) was represented by an array of wooden dowels, which was based on dune vegetation samples collected by Feagin et al. (2019). The species of interest were *Ammophila breviligulata, Uniola paniculata*, and *Panicum amarum* because these are three dominant pioneer dune grass species found along the Atlantic and Gulf of Mexico, regions frequently threatened by tropical and extratropical storms. The reported average stem densities were 93 stems/m^2 for *A. breviligulata*, 72 stems/m^2 for *U. paniculata*, and 76.8 stems/m^2 for *P. amarum*. The average stem diameters for the three species were 3.38, 3.83, and 5.9 mm, respectively. For a vegetation canopy approximated by circular cylinders, the canopy density can be described by the nondimensional solid volume fraction *Φ*, defined by Nepf (2012) as:

$$\phi = \left(\frac{\pi}{4}\right) N d^2 \tag{2}$$

where d is the plant diameter and N is stem density. The average solid volume fraction for the three species of interest was 0.001254. Using a standard dowel diameter of 3.175 mm (⅛ inch), the target density to obtain the desired volume fraction was 158 stems/m^2, which corresponds to a grid spacing of 8.0 cm. The 30.5-cm long dowels were installed on a staggered grid extending the entire width of the flume (1.5 m) in the alongshore and 1.0 m in the cross-shore from the sloping wall along the dune crest, totaling 229 dowels. The burial depth of each dowel into the sand was 15.25 cm to limit uprooting. Wooden dowels do not have the structural properties of flexible dune vegetation, but given the shallow water depths impacting the dune, the dowels should provide comparable blockage area, flow separation, and erosion patterns.

The belowground biomass in established dunes are in a symbiotic association with arbuscular mycorrhizal (AM) fungi (Koske and Polson, 1984). The symbiotic AM fungi provide a web of non-soluble hyphae that provides nutrients for vegetation roots in exchange for carbohydrates. Together, roots and hyphae bind sand into aggregates (Tisdall and Oades, 1982) that may reduce erosion and transport rates. Belowground biomass in the beach-dune model was represented by natural coconut husk fibers or coir. No attempt to mimic the binding of sediment via hyphae was attempted in the laboratory, although the coir was observed capturing the sediment during the experiments, as shown in Fig. 3. Measured belowground biomass considering 12 different dune vegetation species was obtained from Feagin et al. (in review). Collected within a 0.075 m^3 volume, the average belowground mass density considering all species was 2350 g/m^3. Typically, coastal Froude similitude models use water as their liquid medium resulting in a density ratio between the model and prototype equal to one (Hughes, 1993). The choice was made to model the density of the belowground biomass in the model as it was measured in the prototype to maintain this density ratio, however the coir fibers individually were not scaled to any plant root or biomass metrics. This density was approximated in the experiment by mixing 300 g of coir with 0.126 m^3 of dry sand, resulting in a laboratory belowground biomass density of 2380 g/m^3. No attempt was made to provide a physical connection between the above and belowground biomass to assess the contribution of the vegetation structures in reducing erosion both separately and together. To add the belowground biomass, sand from the dune, designated as that above the sloping back wall, was removed, weighed, and uniformly integrated with the coir using a concrete mixer. This sand-coir substrate was then

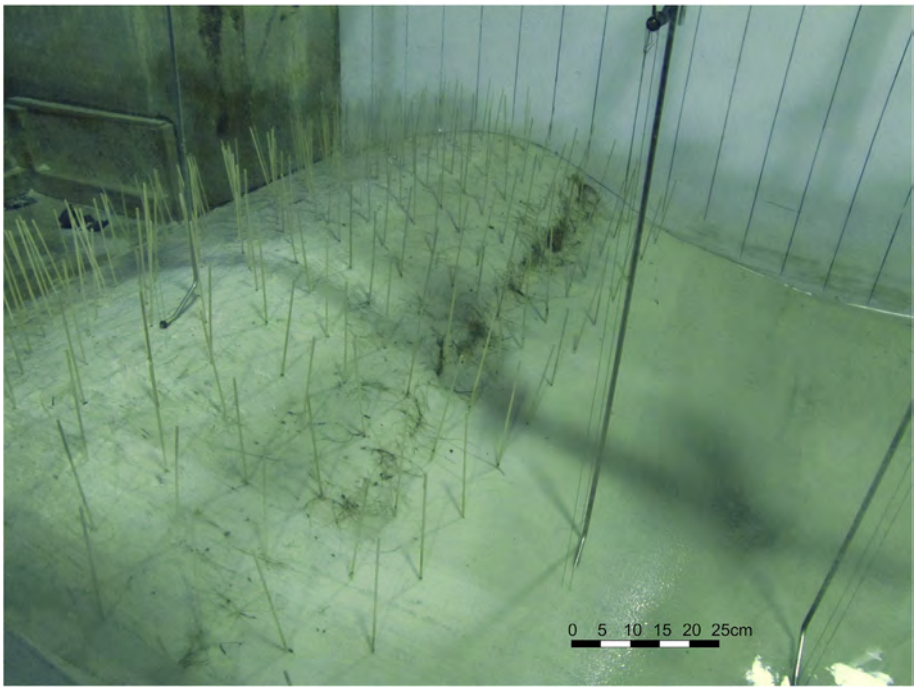

Fig. 2. Picture of beach-dune model with incorporated biomass.

returned to the flume and molded to the dune profile. Modeled dune vegetation covers and their corresponding notation are provided in Table 2.

2.4. Lidar

Area lidar (light detection and ranging) scans were used to capture high resolution geometric data of the total change in dune profile before and after each wave burst. The lidar system used was a RIEGL LMS-390(i) terrestrial laser scanner, which has an accuracy of 6 mm in the horizontal and the vertical at 300 m. The vertical and horizontal scanning ranges are 50–130° and 0–360°, respectively. The lidar was mounted at a fixed location above the wave flume on the landward side of the dune and tilted downward 25° on its mount to scan the dune-beach model. A local coordinate system was established using 12 tie-points to geo-reference each individual scan to the same reference plane

Table 2
Modeled dune vegetation covers.

Cover ID	Aboveground	Belowground
Control	None	None
A	153 stems/m^2	None
B	None	2380 g/m^3
AB	153 stem/m^2	2380 g/m^3

Fig. 3. Picture showing sediment binding with coir fibers.

to expedite both collection and processing. These tie-points were reflective targets with an associated x-, y-, and z-centroid location and were located prior to each hydrodynamic test through a panoramic (angle measurement resolution of 0.001 deg) pre-test scan (resolution of 0.12 arc seconds). Once located in the panoramic scan, each target was fine scanned at 0.001 arc seconds to provide a precise location of the target centroids. During data processing, the respective target centroids were then adjusted to the position of the associated tie-points. The area lidar scans captured the dune and a 2–3 m portion of the beach, measured seaward from the center of the dune, with an angle measurement resolution of 0.001 deg and a spatial resolution of 0.05 arc seconds. These high resolution area scans provided pre- and post-wave dune and beach geometry following each burst.

2.5. Methodology

To approximate the same beach-dune profile for each test, the dune form was constructed by hand molding sand according to permanent guidelines along each flume wall. The pre-scan was collected for the dune and beach prior to filling the wave flume. The flume was then filled slowly to the correct SWL over 2 h to assure no sediment moved during filling. Once filled, sampling by the wave gauges was initiated followed by a wave burst. Upon completion of a wave burst, the water in the flume was slowly drained to minimize sediment transport during dewatering and a post-scan collected. In addition, the following steps were completed between each wave burst: 1) sediment and water captured in the overwash catch basin was removed, allowed to dry, and weighed, 2) uprooted and felled wooden dowels were removed, and 3) belowground biomass floating free of the dune was removed (belowground biomass simply exposed by wave attack was not disturbed as it remained partially integrated with the dune). When aboveground biomass was present, two post-scans were collected following the final wave burst, one with and one without the wooden dowels. In this instance, the wooden dowels were removed carefully by hand to reduce impact on the dune morphology.

3. Results

3.1. Beach-dune profile response

The elevations of the beach-dune model were averaged alongshore following each wave burst to obtain single profiles as a function of x, where $x = 0$ is the landward end of the dune at the sloping wall of the sand trap. The alongshore profiles were averaged in 0.5 cm bins over a width slightly smaller than the flume, approximately 1.4 m, to omit edge effects along the flume walls. The vertical coordinate z was defined positive upwards with $z = 0$ at the shallow SWL. The analysis was limited to the zone x = 0–2 m because this area showed the most active evolution.

The pre- and post-measured dune profiles following the series of wave bursts for the collision regime conditions SC1, SC2, and DC are shown in the top panels of Fig. 4. The bottom panels show the difference in elevation between the final profiles of the vegetated dunes and the control dune. In both the SC1 and SC2 cases, material was eroded primarily from the dune face and redistributed as to steepen the nearshore beach to a common slope of approximately 12°. However, whereas SC1 saw scarping in the zone x = 0.5–0.7 m, scarping was observed further seaward at x = 0.7–0.9 m for SC2. Looking at the bottom panel of SC1, the amount of erosion relative to the control varied, depending on the presence and type of biomass. Less scarping of the dune face was observed in the presence of biomass, regardless of form. The A vegetation cover had the smallest impact, around 1 cm of positive elevation, whereas the B and AB vegetation covers retained about 4 cm of elevation compared to the control. Unlike SC1, the existence of biomass had negligible effects on the dune response compared to the control for SC2.

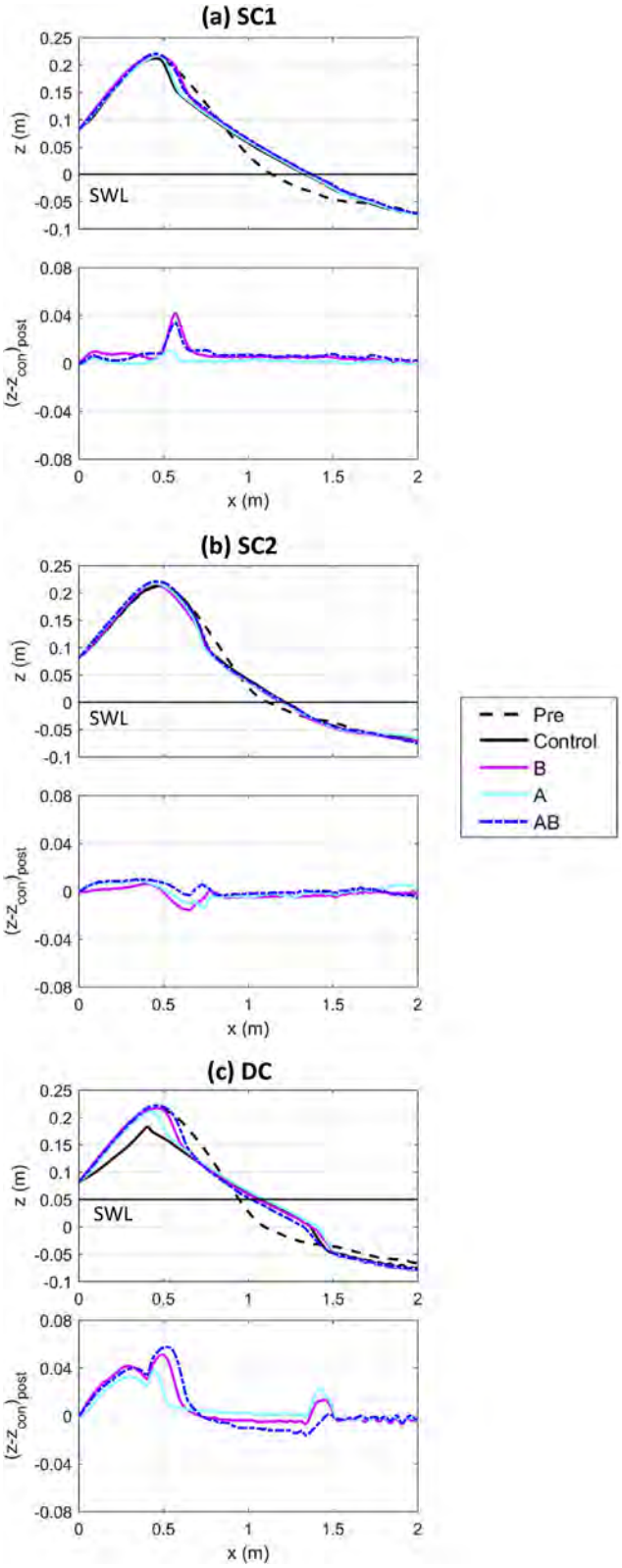

Fig. 4. Profile evolution (top panel) and difference in final profiles between the control and the aboveground only (A), belowground only (B), and aboveground and belowground (AB) vegetation covers (bottom panel) for the SC1 (a), SC2 (b), and DC (c) collision.

Similar to SC1 and SC2, the final profile of DC exhibited a single beach slope of approximately 12° leading from the dune to the submerged portion of the profile for all vegetation covers. However, unlike

the SC tests, sediment was deposited offshore to form a small bar near x = 1.5 m as seen in the bottom panel of Fig. 4c. The erosion of the beach-dune model during the DC test was more severe than SC1 and SC2, especially for the control dune. The extensive erosion of the crest and lee slope of the control dune resulted from an increase in wave overtopping due to the continuous undermining of the dune face in conjunction with deeper water, ultimately changing the regime from collision to overwash. Erosion was significantly reduced in the presence of biomass. These differences in the dune response between the control and the vegetated dunes is illustrated by the double arch shape evident in the bottom panel of Fig. 4c in the zone x = 0.0–0.7 m. Whereas the crest of the control dune was eroded by nearly 5 cm, the dunes with biomass retained the crest elevation and only experienced scarping of the dune face. The degree of scarping depended on the biomass type, where the AB vegetation cover experienced the least amount, followed by the B vegetation cover, and then the A vegetation cover. This trend is illustrated by the successive lowering and retreat of the maximum elevation difference near x = 0.5 in the bottom panel of Fig. 4c. Additionally, the dunes with biomass retained elevations along the lee slope similar to that of the initial profile, indicating that the presence of biomass, regardless of form, delayed the onset of overtopping.

The pre- and post-measured dune profiles following the series of wave bursts for the overwash regime conditions SO and DO are shown in the top panels of Fig. 5. The bottom panels show the difference in elevation between the final profiles of the vegetated dunes and the control dune. Despite the differences in water depth and design regime, the dune response of the SO test was similar to the DC test. The difference in dune response between the control dune and the dunes with biomass in both experiments is characterized by a double arch shape in x = 0.0–0.7 m, indicating a reduction in erosion of the dune face and along the lee slope in the presence of vegetation. Again, the degree of erosion depended on the biomass form. The AB vegetation cover experienced the least erosion of the dune face and lee slope, followed in ascending order by B and A. The beach profile saw less deposition at the base of the stoss slope than the control for B and AB, as indicated by the negative values in the bottom panel of Fig. 5a, because less sediment was transported from the dune.

The most severe erosion of the control dune-beach model was observed during the DO test. As seen in the top panel of Fig. 5b, the control dune experienced dramatic erosion very rapidly by beginning in the overwash regime. The bottom panel of Fig. 5b shows that the presence of biomass, particularly belowground, has significant impact on the dune response. Whereas the entire control dune was nearly flattened following one wave burst, a dune profile is clearly evident for the B and AB vegetation covers. It is important to note that the shown

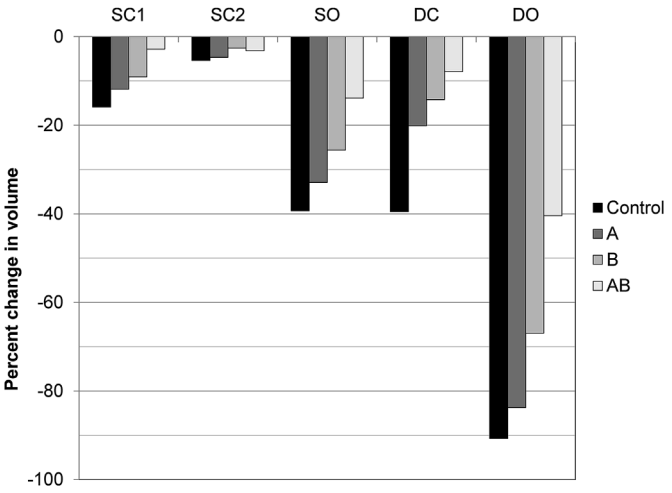

Fig. 6. Percent change in volume between pre and post surveys for all modeled hydrodynamic conditions and vegetation covers.

profile of the AB dune is following three wave bursts whereas the control, B, and A is following one wave burst. The AB dune was significantly more resistant to erosion than the other conditions and required additional wave bursts to initiate erosion. The AB, B, and A vegetation covers have a maximum elevation of about 9.0 cm, 5.0 cm, and 2.0 cm above the control, respectively.

3.2. *Changes in volume and overwash*

To calculate the change in volume, only the top portion of the dune, that above the sand trap wall, was considered since this sediment was incorporated with belowground biomass. The dune was consistently eroded in all the tests and, thus, the percent change in erosion from the pre to the post surveys are all negative values, as shown in Fig. 6. The greatest loss of sand always occurs under the control conditions, with a percent decrease in volume ranging from a minimum of −5.4% for SC2 to a maximum of −90.7% for DO. The presence of biomass, regardless of form, reduced the volume of material loss from the dune for all modeled hydrodynamic conditions. Furthermore, dunes with belowground biomass, either in isolation or in combination with aboveground biomass, resisted erosion better than dunes with only aboveground biomass. Except for SC2, which experienced the least erosion overall, the percent loss in material volume was the smallest under the AB vegetation cover for all hydrodynamic conditions (−2.8% for SC1,

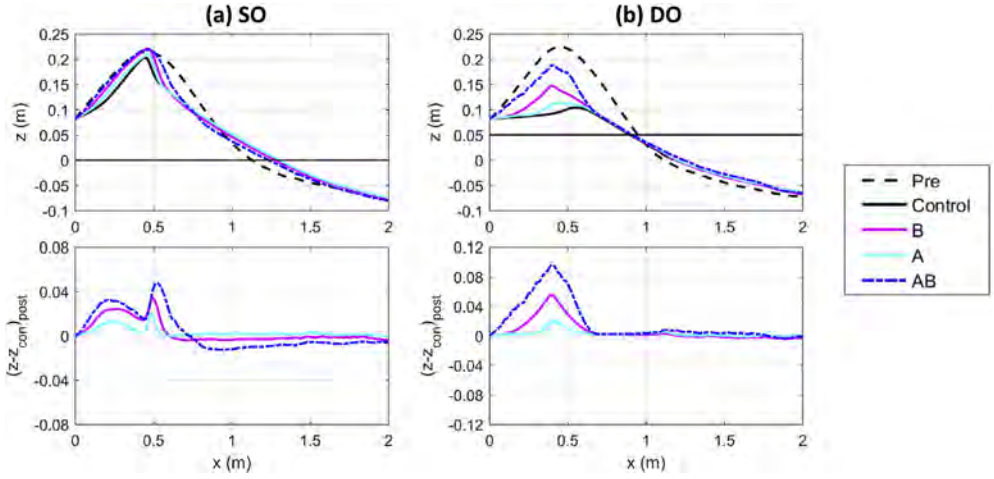

Fig. 5. Profile evolution (top panel) and difference in final profiles between the control and the aboveground only (A), belowground only (B), and aboveground and belowground (AB) vegetation covers (bottom panel) for the SO (a) and DO (b) overwash regimes.

Table 3
Amount of sediment and water over wash for DC, SO and DO hydrodynamic conditions.

Deep Collision	Control	A	B	AB
Total Water (kg)	13.6	Nominal	0	0
Total Sediment (kg)	15.0	3.6	0	0
Percent of Overwash Sediment to Total Dune Mass	7%	2%	0%	0%
Percent Decrease in Sediment Loss to Overwash Versus Control		76%	100%	100%
Shallow Overwash	**Control**	**A**	**B**	**AB**
Total Water (kg)	49.3	59.4	30.8	Nominal
Total Sediment (kg)	37.6	24.9	15.9	5.4
Percent of Overwash Sediment to Total Dune Mass	17%	12%	7%	3%
Percent Decrease in Sediment Loss to Overwash Versus Control		34%	58%	86%
Deep Overwash	**Control**	**A**	**B**	**AB**
Total Water (kg)	464	527.1	356.1	108.0
Total Sediment (kg)	144.2	115.5	78.0	24.9
Percent of Overwash Sediment to Total Dune Mass	67%	53%	36%	12%
Percent Decrease in Sediment Loss to Overwash Versus Control		20%	46%	83%

-13.9% for SO, −7.9% for DC, and −40.4% for DO). For the DO-AB condition, the percent loss in material was less than half of that observed for the control dune even after three wave bursts.

Following each wave burst, the water and sediment overwash resulting from wave runup and overtopping was collected and weighed. The total water overwash weight, total sediment overwash, both weight and percent relative to total dune mass, and the percent decrease in sediment overwash relative to the control is given in Table 3 for the DC, SO, and DO conditions. The overwash for the SC1 and SC2 conditions was extremely small and is not reported here. The DO hydrodynamic condition saw an increase in total sediment and total water overwash compared to the SO hydrodynamic condition; the sediment overwash was 3.8–4.9 times higher and the water overwash was 8.8–11.5 times higher than that measured for the SO condition considering all vegetation covers, including the control. Repeating the trend observed in the volume calculations, there is a decrease in the sediment overwash compared to the control dune as one progresses through the aboveground, belowground, and aboveground and belowground vegetation covers for all hydrodynamic conditions. For the DC condition, the control dune lost 7% of its mass in sediment overwash compared to 2% for the aboveground only and 0% for both covers the included belowground biomass (B and AB). The amount of water overwash for DC was nominal in the presence of biomass compared to 13.6 kg for the control. The percent of overwashed sediment relative to the dune mass for the SO condition decreased from 17% for the control dune to 12% for A, 7% to B, and 3% to AB. The change in water overwash for the same condition compared to the control was +20%, −38%, and −100%, respectively. The decrease in sediment and water overwash for the DO condition is more substantial. The control dune lost 67% of its sediment mass as overwash compared to 53%, 36%, and 12%, with change in water overwash of +13%, −23%, and −77% for A, B, and AB, respectively. The sediment overwash decreased with all vegetation covers, but the water overwash increased for the A vegetation cover, similarly to the SO condition. Kobayashi et al. (2013) also observed an increase in the wave overtopping rate and overwash volume for a dune constructed with model vegetation only along the lee slope. Unlike a natural dune system, where plants grow at irregular spacing, both this study and Kobayashi et al. (2013) placed wooden dowels in a regular pattern. This construction method may have created preferential paths for the overwash, increasing the mass of water in the SO and DO conditions for the A vegetation cover. The percent decrease in sediment overwash relative to the control for both the SO and DO conditions was similar across like vegetation covers. The A vegetation cover reduced the sediment overwash 34% and 20% for the SO and DO conditions. Comparing the B vegetation cover for the SO and DO conditions show the same trend, with sediment overwash decreasing 58% and 46%. The AB vegetation cover saw a reduction in the sediment overwash of 86% and 83%. Due to the limited testing matrix, this similarity in the measured sediment overwash reduction independent of hydrodynamic condition across vegetation covers requires further investigation.

4. Conclusions

A laboratory study of a scaled dune-beach system was conducted to investigate whether, and to what degree, vegetation alters the dune response to collision and overwash wave attack regimes. A dune profile, with and without the presence of artificial dune vegetation, was subjected to five wave conditions in a large-scale wave flume. Previous studies demonstrated that the presence of vegetation reduces the erosion of dunes and results in a higher post storm dune height, but these studies did not consider belowground biomass (Kobayashi et al., 2013) or did not measure it (Figlus et al., 2014; Silva et al., 2016). Based upon recommendations of these previous studies, both aboveground (e.g., stems) and belowground (e.g., roots) biomass were simulated, both in isolation and in combination, in order to quantify the dominant mechanisms contributed by vegetation structure to dune response (e.g., stems vs roots). The aboveground and belowground biomass quantities were modeled in this study at levels measured in situ. Overall, the results showed that vegetation biomass, regardless of form, reduces the degree of erosion sustained during collision and overwash impact regimes. For the collision regime, biomass reduced scarping of the dune face at lower water levels and delayed the onset of overtopping and transition to the overwash regime at deeper water levels. For the overwash regime, the presence of biomass reduced erosion of the dune's lee and stoss slope, and, in the case of the deeper water level, prevented the flattening of the entire dune form.

These results not only reinforce the important role of vegetation in dune stabilization, but begin to address the nonlinear interactions between the vegetation and the dune response. As expected, the combination of above and belowground biomass, which best represents live vegetation, resulted in the lowest percent loss of dune material and the greatest percent decrease in sediment and water overwash compared to the bare, control dune. Looking at the isolated biomass, there was a much greater dune resistance afforded by the isolated belowground biomass compared to the isolated aboveground biomass, likely due to the difference in the physical mechanisms by which vegetation alters the degree of erosion. The aboveground biomass dissipates wave energy by increased friction and turbulence whereas the belowground biomass binds and reinforces the soil. Additionally, observations during the experiment showed that dislodged belowground biomass accumulated at the toe of the dune, which significantly reduced wave uprush velocity and excursion. This reduction in overtopping is reflected in the significant decrease in sediment and water overwash for vegetation covers, particularly those including belowground biomass compared to the isolated aboveground biomass and control dune.

While this study improves our mechanistic understanding of the role of vegetation in dune systems, it also demonstrates the level of difficulty in mimicking real vegetation, and their effects in a laboratory setting. This study did not consider the connection between the below and aboveground biomass thus not capturing the uprooting process that may occur during high energy events. In agreement with previous studies, more field observations are needed. For example, as part of these efforts, it is important to consider the maturity of the vegetation-dune system. This effort is representative of more mature, natural dune systems, where vegetation is well established and biomass is

incorporated extensively throughout the dune form. Conversely, dunes constructed and rehabilitated as of part of beach nourishment projects are typically built to the desired elevation and then planted with vegetation (e.g., the dunes are not allowed to build naturally). These man-made dunes are anticipated to be less resistant than a natural dune of the same elevation given that the plants are not yet established and have not gone through multiple burial lifecycles. This natural building process results in greater compaction with dunes having higher levels of organic matter and grain-to-grain cohesion (Feagin et al., 2015). Oftentimes, there is not enough time to wait for dunes to rebuild naturally, which can take a decade a more. The lack of measured data for the biomass distribution in dunes highlights the need to measure the ecological difference between natural and constructed dune systems. Additionally, innovative dune construction methods that incorporate organic fibers or other forms of biomass may increase the stability of dunes undergoing wave attack, providing increased coastal protection. However, as the incorporation of biomass may reduce the survivability and growth of the desired vegetation and impact the dune fauna in ways we as yet do not understand, resulting in unintended negative consequences and feedbacks, monitoring and evaluation of constructed dunes built with added biomass is critical.

Acknowledgements

Funding support was provided by US Army Corps of Engineer's Flood and Coastal Systems Program led by Dr. Julie Rosati and Ms. Mary Cialone, Coastal Inlets Research Program led by Ms. Tanya Beck, and the Engineering with Nature Initiative within the Dredging Operations and Environment Research Program led by Dr. Todd Bridges. Marshall Thomas and William Henderson provided laboratory support. The authors would also like to thank the reviewers for their time and input.

Appendix A. Supplementary data

Supplementary data to this article can be found online at https://doi.org/10.1016/j.coastaleng.2019.103506.

References

Anderson, M.E., Smith, J.M., 2014. Wave attenuation by flexible, idealized salt marsh vegetation. Coast. Eng. 83, 82–92.
Arens, S.M., 1996. Patterns of sand transport on vegetated foredunes. Geomorphology 17, 339–350.
Arens, S.M., Baas, A.C.W., Van Boxel, J.H., Kalkman, C., 2001. Influence of reed stem density on foredune development. Earth Surf. Process. Landforms 26, 1161–1176.
Ayat, B., Kobayashi, N., 2015. Vertical cylinder density and topping effects on dune erosion and overwash. J. Waterw. Port, Coast. Ocean Eng. 141 (1).
Bonham, A.J., 1983. The management of wave-spending vegetation as bank protection against boat wash. Landsc. Plan. 10 (1), 15–30.
Borsje, B.W., van Wesenbeeck, B.K., Dekker, F., Paalvast, P., Bouma, T.J., van Katwijk, M.M., dr Vries, M.B., 2011. How ecological engineering can serve in coastal protection. Coast. Eng. 37, 113–122.
City of New York, 2013. PlanNYC: a Stronger, More Resilient New York. The City of New York, New York, NY. http://www.nyc.gov/html/sirr/html/report/report.shtml.
Davidson-Arnott, R.G.D., 2005. Conceptual model of the effects of sea level rise on Sandy coast. J. Coast. Res. 21 (6), 1166–1172.
Davidson-Arnott, R., 2010. Introduction to Coastal Processes and Geomorphology. Cambridge University Press, New York, USA.
Dean, R.G., Dalrymple, R.A., 2004. Coastal Processes with Engineering Applications. Cambridge University Press, New York, USA.
Donnelly, C., Kraus, N., Larson, M., 2006. State of knowledge on measurement and modeling of coastal overwash. J. Coast. Res. 22 (4), 965–991.
Feagin, R.A., Figlus, J., Zinnert, J.C., Sigren, J., Martínez, M.L., Silva, R., Smith, W.K., Cox, D., Young, D.R., Carter, G., 2015. Going with the flow or against the grain? The promise of vegetation for protection beaches, dunes, and barrier islands from erosion. Front. Ecol. Environ. 13 (4), 203–210.
Feagin, R.A., Furman, M., Salgado, K., Martinez, M.L., Innocenti, R.A., Eubanks, K., Figlus, J., Huff, T.P., Sigren, J., Silva, R., 2019. The role of beach and sand dune vegetation in mediatingwave run up erosion. Estuar. Coast Shelf Sci. 219, 97–106.
Figlus, J., Kobayashi, N., Gralher, C., Iranzo, V., 2011. Wave overtopping and overwash of dunes. J. Waterw. Port, Coast. Ocean Eng. 137 (1), 26–33.
Figlus, J., Sigren, J.M., Armitage, A.R., Tyler, R.C., 2014. Erosion of vegetated coastal dunes. In: Proceedings of the 34th Conference on Coastal Engineering, (Seoul, Korea).
Gedan, K.B., Kirwan, M.L., Wolanski, E., Barbier, E.B., Silliman, B.R., 2011. The present and future role of coastal wetlands vegetation in protection shorelines: answering recent challenges to the paradigm. Clim. Change 106 (1), 7–29.
Goda, Y., Suzuki, Y., 1976. Estimation of incident and reflected waves in random wave experiments. In: Proc. 15th Intern. Coast. Eng. Conf. ASCE, pp. 828–845.
Hanley, M.E., Hoggart, S.P.G., Simmonds, D.J., Bichot, A., Colangelo, M.A., Bozzeda, F., Heurtefeux, H., Ondiviela, B., Ostrowski, R., Recio, M., Trude, R., Zawadzka-Kahlau, E., Thompson, R.C., 2014. Shifting sands? Coastal protection by sand banks, beaches, and dunes. Coast. Eng. 87, 136–146.
Hesp, P., 2002. Foredunes and blowouts: initiation, geomorphology and dynamics. Geomorphology 48, 245–268.
Hughes, S.A., 1993. Physical Models and Laboratory Techniques in Coastal Engineering. World Scientific Publishing Co., River Edge, NJ, USA.
Keijsers, J.G.S., Giardino, A., Poortinga, A., Mulder, J.P.M., Riksen, M.J.P.M., Santinelli, G., 2015. Adaptation strategies to maintain dunes as flexible coastal defense in The Netherlands. Mitig. Adapt. Strategies Glob. Change 20, 913–928.
Keijsers, J.G.S., De Groot, A.V., Riksen, M.J.P.M., 2016. Modeling the biogeomorphic evolution of coastal dunes in response to climate change. J. Geophys. Res.: Earth Surf. 121, 1161–1181.
Knutson, P.L., 1977. Plant Guidelines for Dune Creation and Stabilization. U.S. Army Corps of Engineers: Coastal Engineering Research Center, Fort Belvoir, VA Coastal Engineering Technical Aid No. 77-4.
Kobayashi, N., Gralher, C., Do, K., 2013. Effects of woody plants on dune erosion and overwash. J. Waterw. Port, Coast. Ocean Eng. 139 (6), 466–472.
Koske, R.E., Polson, W.R., 1984. Are VA Mycorrhizae required for sand dune stabilization? Bioscience 34 (7), 420–424.
Kraus, N.C., Smith, J.M., 1994. Main Text. SUPERTANK Laboratory Data Collection Project, vol. 1 U. S. Army Corps of Engineers Technical Report CERC-94-3.
Miller, R.M., Jastrow, J.D., 1990. Hierarchy of root and mycorrhizal fungal interactions with soil aggregation. Soil Biol. Biochem. 22 (5), 579–584.
Nepf, H.M., 2012. Flow and transport in regions with aquatic vegetation. Annu. Rev. Fluid Mech. 44, 123–142.
National Oceanic and Atmospheric Administration (NOAA), 2013. National Coastal Population Report: Population Trends from 1970 to 2020. Silver Spring, Maryland.
Pollen, N., 2007. Temporal and spatial variability in root reinforcement of streambanks: accounting for soil shear strength and moisture. Catena 69 (3), 197–205.
Sallenger Jr., A.H., 2000. Storm impact scale for barrier islands. J. Coast. Res. 16, 890–895.
Sigren, J.M., Figlus, J., Armitage, A.R., 2014. Coastal sand dunes and dune vegetation: restoration, erosion, and storm protection. Shore Beach 82 (4), 5–12.
Silva, R., Martínez, M.L., Odériz, I., Mendoza, E., Feagin, R.A., 2016. Response of vegetated dune-beach systems to storm conditions. Coast Eng. 109, 53–62.
Texas General Land Use Office, 2005. Dune Protection and Improvement Manual for the Texas Gulf Coast, fifth ed. .
Tisdall, J.M., Oades, J.M., 1982. Organic matter and water-stable aggregates in soils. J. Soil Sci. 33, 141–163.
Tomasicchio, G.R., Sánchez-Arcilla, A., D'Alessandro, F., Ilic, S., James, M.R., Sancho, F., Fortes, C.J., Schüttrumpf, H., 2011. Large-scale experiments on dune erosion processes. J. Hydraul. Res. 49 (S1), 20–30.
U.S. Army Corps of Engineers (USACE), 2013. Hurricane Sandy Coastal Projects Performance Evaluation Study, Disaster Relief Appropriations Act, 2013. Submitted by the Assistant Secretary of the Army for Civil Works, November 6, 2013.
Van Rijn, L.C., 2009. Prediction of dune erosion due to storms. Coast. Eng. 56, 441–457.
Van Slobbe, E., de Vriend, H.J., Aarninkhof, S., Lulofs, K., de Vries, M., Dircke, P., 2013. Building with Nature: in search of resilient surge protection strategies. Nat. Hazards 65, 947–966.
Van Thiel de Vries, J.S.M., van Gent, M.R.A., Walstra, D.J.R., Reniers, A.J.H.M., 2008. Analysis of dune erosion processes in large-scale flume experiments. Coast. Eng. 55 (12).
Veylon, G., Ghestem, M., Stokes, A., Bernard, A., 2015. Quantification of mechanical and hydric components of soil reinforcement by plant roots. Can. Geotech. J. 52 (11), 1839–1849.
Walling, K., Miller, J.K., Herrington, T.O., Eble, A., 2014. Comparison of Hurricane Sandy impacts in three New Jersey coastal communities. In: Proceedings of the 34th Conference on Coastal Engineering, Seoul, Korea).
Williams, M.J., 2007. Native Plants for Coastal Restoration: what, when, and How for Florida. USDA, NRCS, Brooksville Plant Materials Center, Brooksville, FL 51pp.. http://www.fl.nrcs.usda.gov/programs/pmc/flplantmaterials.html.

REPORT DOCUMENTATION PAGE

Form Approved
OMB No. 0704-0188

1. REPORT DATE *(DD-MM-YYYY)*	2. REPORT TYPE	3. DATES COVERED *(From - To)*
August 2021	Final	

4. TITLE AND SUBTITLE

The Response of Vegetated Dunes to Wave Attack

5a. CONTRACT NUMBER

5b. GRANT NUMBER

5c. PROGRAM ELEMENT NUMBER

6. AUTHOR(S)

Duncan B. Bryant, Mary Anderson Bryant, Jeremy A. Sharp, Gary L. Bell, and Christine Moore

5d. PROJECT NUMBER

5e. TASK NUMBER

5f. WORK UNIT NUMBER

7. PERFORMING ORGANIZATION NAME(S) AND ADDRESS(ES)

Coastal and Hydraulics Laboratory
U.S. Army Engineer Research and Development Center
3909 Halls Ferry Road
Vicksburg, MS 39180

8. PERFORMING ORGANIZATION REPORT NUMBER

ERDC/CHL MP-21-4

9. SPONSORING / MONITORING AGENCY NAME(S) AND ADDRESS(ES)

U.S. Army Corps of Engineers
Washington, DC 20314

10. SPONSOR/MONITOR'S ACRONYM(S)

11. SPONSOR/MONITOR'S REPORT NUMBER(S)

12. DISTRIBUTION / AVAILABILITY STATEMENT

Approved for public release; distribution is unlimited.

13. SUPPLEMENTARY NOTES

This article was originally published online in *Coastal Engineering* on 13 May 2019.
Funding was under the USACE Flood and Coastal Systems Program, the Coastal Inlets Research Program, and the Engineering with Nature Initiative within the Dredging Operations and Environment Research Program.

14. ABSTRACT

Vegetation is believed to increase the stability of dunes during wave attack, but limited data is available. A physical model study was performed to evaluate changes in the dune stability with and without biomass, both above and belowground. The above and belowground biomass was modeled using wooden dowels and coir fibers, respectively. For both the collision and overwash storm impact regimes, the results of this study clearly demonstrate that the inclusion of biomass in the model dune reduces the erosion and overwash. The combination of both above and belowground biomass was the most effective at reducing erosion followed by belowground biomass, with aboveground biomass providing the smallest benefit regardless of the wave condition and water level. Additionally, the overwash of sediment and water was decreased with the inclusion of biomass, following the same trends as the erosion. As the dune eroded, the storm impact regime transitioned from collision to overwash. The inclusion of biomass delays this transition in storm impact regime, providing greater protection to coastal communities. This study highlights the need to consider dune vegetation for dune construction and coastal planning.

15. SUBJECT TERMS

Dunes; sediment transport; erosion; vegetation; wave overtopping; overwash

16. SECURITY CLASSIFICATION OF:			17. LIMITATION OF ABSTRACT	18. NUMBER OF PAGES	19a. NAME OF RESPONSIBLE PERSON
a. REPORT	b. ABSTRACT	c. THIS PAGE			19b. TELEPHONE NUMBER *(include area code)*
Unclassified	Unclassified	Unclassified	UU	13	